Christoph Günster (Autor)

Magnetically and Capillary Driven Grain Boundary Motion in Zinc Bicrystals

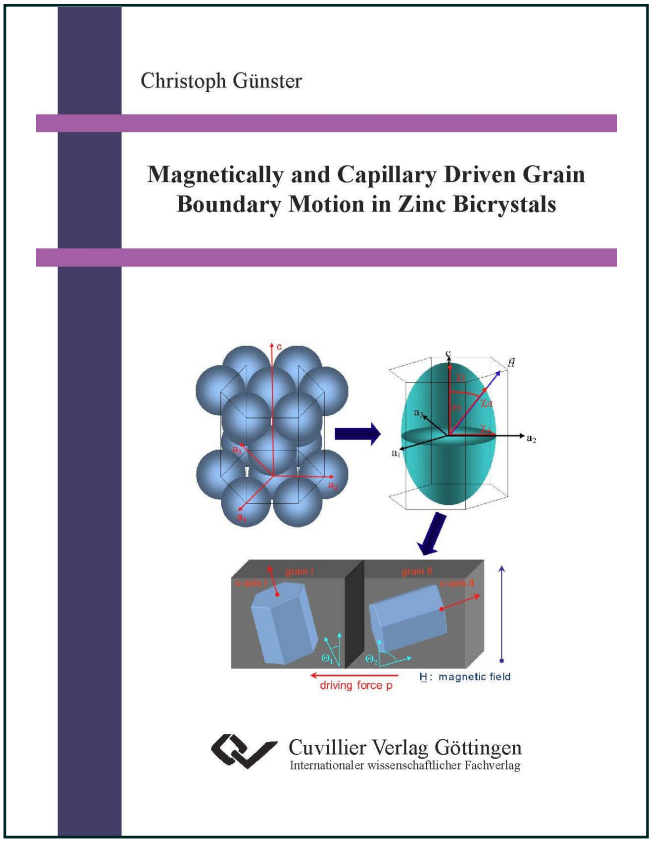

https://cuvillier.de/de/shop/publications/6398

1. Fundamentals of grain boundaries and grain boundary migration

1.1. Introduction

The properties of crystalline metallic materials are determined by their deviation from a perfect crystal lattice, which occurs due to their intrinsic crystal defects. Without those crystal defects, metals would never have been used in such a wide variety of applications [2]. There are different types of crystal defects which are distinguished by their spatial dimension. One of the longest known and most important defects in metals is the grain boundary, a two-dimensional planar defect, which separates two adjacent crystallites of the same crystal structure and chemical composition, but of different orientation [1]. Since any crystalline material, except for single crystals, is granular-structured, grain boundaries are the fundamental defect in polycrystalline materials, exerting a substantial impact on their properties [2].

1.2. Classification

In three-dimensional space, there are eight degrees of freedom, which means eight independent parameters are required to assign a mathematically exact definition to a given grain boundary [9]. Three parameters are necessary to define the orientation relationship between two adjacent grains which are usually represented by an Euler angle triplet (φ_1, Φ, φ_2), by Miller indices or by an angle-axis pair in Rodrigues-Frank space [2, 3, 4].

Two more parameters are needed to define the spatial orientation of the grain boundary plane, i.e. the boundary inclination, which are expressed by the normalized crystallographic normal vector of the plane of inclination $\mathbf{n} = (n_1, n_2,$

n_3) with respect to one of the adjacent grains. Additional to these five macroscopic parameters there are three independent values of the microscopic translational vector **t** = (t_1, t_2, t_3) [2]. All intrinsic properties of grain boundaries, particularly mobility and energy, are functions of these eight parameters [1]. The five macroscopic parameters may be influenced externally, whereas the translational vector **t** is determined by the minimum of the total energy of the crystal.

To determine the dependence of grain boundary properties on the five macroscopic parameters introduced above, it would be necessary to keep all but one degree of freedom constant and successively vary one free parameter [1, 2]. However, under realistic experimental conditions only one set of parameters may remain at a fixed value. The most common investigation procedure therefore is to change an orientation relationship by varying the rotation angle and keeping the plane of inclination fixed with respect to a reference point or vice versa while preserving one common axis of rotation [1].

1.3. Presentation of misorientations

The misorientation or orientation relationship between two differently oriented crystallites is a spatial transformation applied to one crystal in order to bring both orientations to coincidence [1]. Assuming a common origin for both lattices, this is achieved by a simple rotation of one lattice relative to the other, which is conveniently expressed by a rotation transformation matrix g^m:

$$\{C_i\} = g^m \{C_j\} \tag{1.1}$$

where $\{C_i\}$ and $\{C_j\}$ are the crystal coordinate systems. The easiest way to describe such a rotation matrix is in terms of a rotation axis <hkl> common for both lattice coordinate systems and a rotation angle θ (Fig. 1-1), since for many

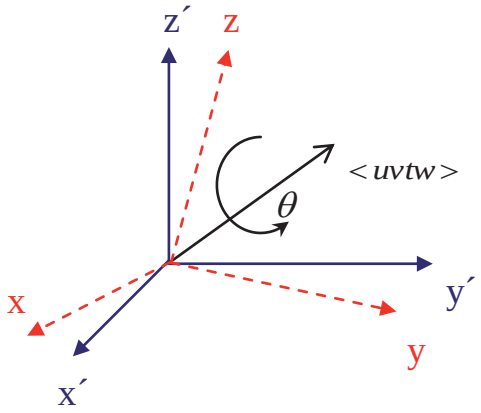

Fig. 1-1: Rotation about axis <*uvtw*> of angle θ brings coordinate system 1 and 2 to coincide.

cases it is of major interest to investigate the influence of the rotation angle on a grain boundary property for a certain rotation axis [1]. Thus, it is common to keep the grain boundary inclination constant and only take into account the rotation angle dependence. Consequently, grain boundaries may be divided into three different categories. In case of a rotation axis perpendicular to the grain boundary plane, the grain boundary is given the denotation twist boundary (Fig. 1-2 a). For this type of grain boundary the grain boundary plane is exactly defined and independent of the rotation angle. In Figures 1-2 b and 1-2 c the class of tilt grain boundaries is depicted. The major difference to twist

boundaries is that the rotation axis is aligned parallel to the boundary plane [1]. Consequently, an infinite number of possible grain boundary planes exists for a given rotation angle. Further, one distinguishes between two types of grain boundary within the class of tilt boundaries. Under the special conditions that mirror symmetry is satisfied between two adjacent grains, the boundary is labeled as a symmetrical tilt boundary (Fig. 1-2 c). All other configurations are denoted as asymmetrical tilt boundaries (Fig. 1-2 b) [1].

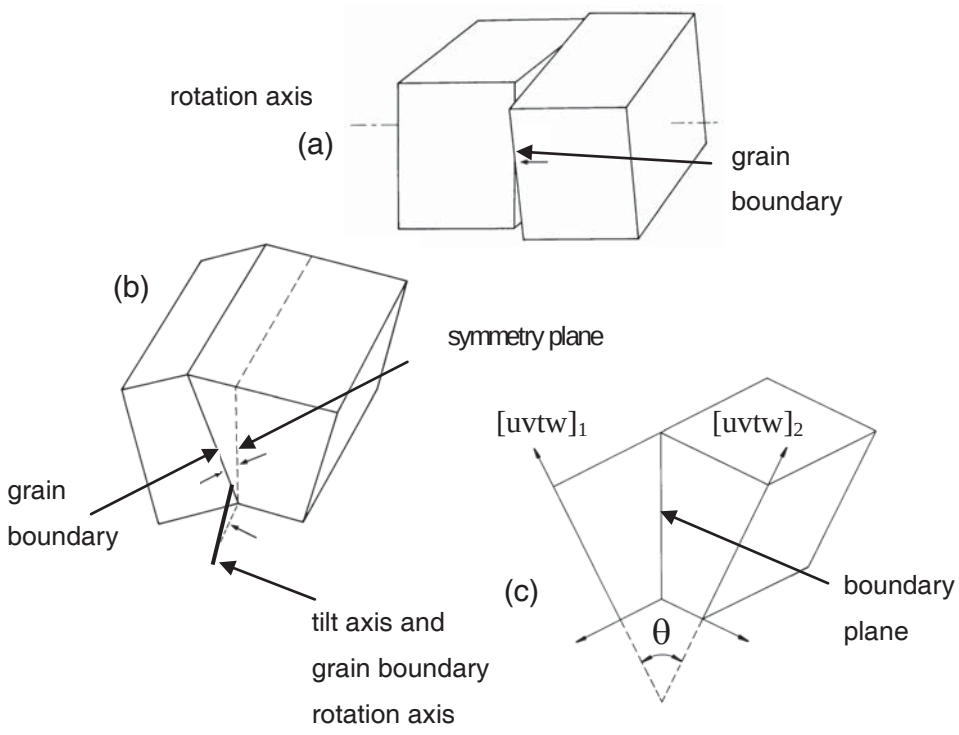

Fig. 1-2: Schematic depictions of a) a twist grain boundary and b) an asymmetrical tilt and c) a symmetrical tilt boundary [1]

Grain boundaries that do not satisfy either of the criteria of the first two classes are termed mixed or random grain boundaries and consist of both twist and tilt components.

1.4. Atomic structure

An additional means to classify grain boundaries is to categorize them, depending on their misorientation, by distinguishing between low angle grain boundaries (LAGBs) and high angle boundaries (HAGBs). In the following sections the difference between these grain boundaries regarding their microstructural configuration will be addressed.

1.4.1. Low angle grain boundaries

Providing the case that the misorientation angle between two neighboring grains is small enough (LAGB), the misorientation of the grain boundary is achieved by lattice distortions introduced by dislocation arrays. In case of a symmetrical $<10\bar{1}0>$ tilt boundary, the configuration consists of a single set of edge dislocations with Burgers vectors $\vec{b}$, where the dislocation spacing directly correlates with the misorientation angle θ (Fig. 1-3a) [1].

$$\frac{|\vec{b}|}{d} = 2\sin\frac{\theta}{2} \tag{2.1}$$

Accompanied with an increasing misorientation angle θ the spacing d decreases as depicted in Fig. 1-3.

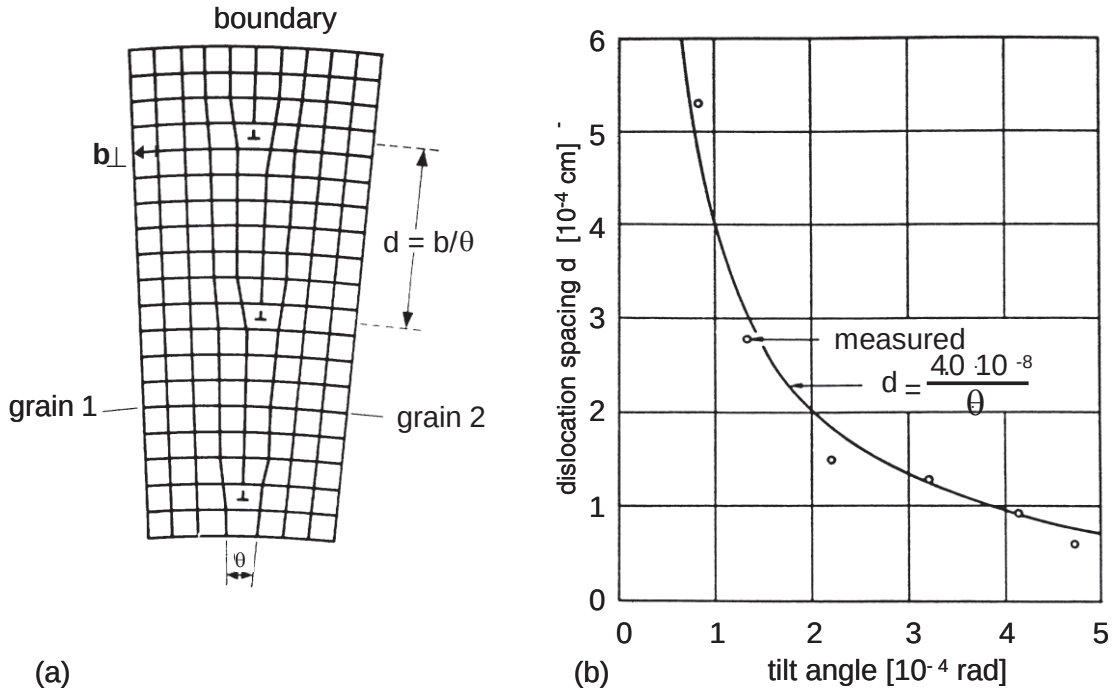

Fig. 1-3: a) Schematic depiction of a symmetrical low angle tilt boundary, b) measured and calculated dislocation spacing versus tilt angle θ in a symmetrical LAGB in Germanium [1]

For asymmetrical tilt grain boundaries (Fig. 1-2 b), in which the boundary plane deviates from its symmetrical position by an inclination angle φ (Fig. 1-4), at least two sets of edge dislocations are necessary to accommodate the boundary configuration. The Burgers vector of these two dislocation sets must be perpendicular to each other (Fig. 1-4 a) and with increasing asymmetry, the fraction of the second set of dislocations ($\vec{b_2}$) has to increase,

$$\frac{1}{d_2} = \frac{\left|\vec{b_2}\right|}{\theta \sin \varphi} \qquad (2.2)$$

while the fraction of dislocations with Burgers vector $\vec{b_1}$ decreases with φ.

a) b)

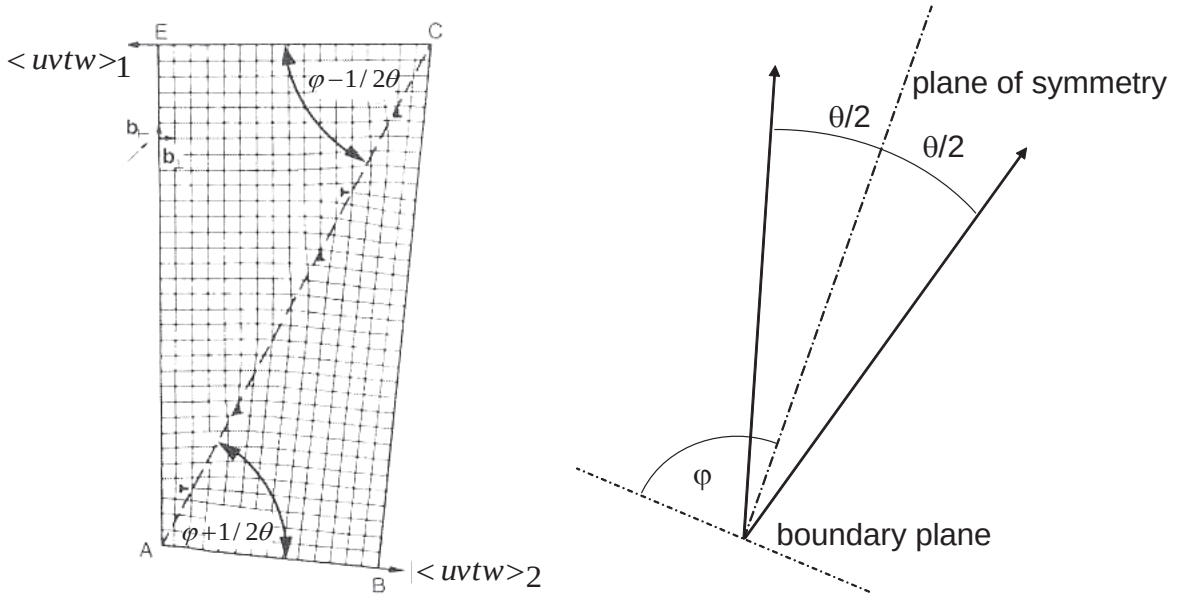

Fig. 1-4: a) Lattice dislocation arrangement [1] and b) rotation angle θ and inclination angle φ of an asymmetrical tilt LAGB.

$$\frac{1}{d_1} = \frac{\left|\vec{b_1}\right|}{\theta \cos\varphi} \tag{2.3}$$

Small angle twist boundaries require two sets of screw dislocations and in the most general case of mixed LAGBs the boundary structure is comprised of dislocation networks of three Burgers vectors [5]. By applying this dislocation model of LAGBs, which was developed by Read and Shockley [6], the exact calculation of free grain boundary energy is possible. As derived by Read and Shockley, the stress field of dislocations in an infinite periodic array is spatially limited to a range of the order of spacing d. In case of an edge dislocation its energy E_d per unit length is thus expressed by:

$$E_d = \frac{\mu b^2}{4\pi(1-\nu)} \ln \frac{d}{r_0} + E_c \qquad (2.4)$$

where ν is the Poisson ratio, μ the shear modulus, $r_0 \approx b$ the radius and E_c the energy of the dislocation core [1]. Keeping in mind, that this equation needs to be applied to a set of dislocations, which compose a LAGB, we introduce the number of dislocations per unit length $n \equiv 1/d = \theta/b$ to the above equation and thereby obtain the energy per unit area for the case of a symmetrical tilt grain boundary:

$$\gamma_b^{symm} = \frac{\theta}{b}\left(\frac{\mu b^2}{4\pi(1-\nu)} \ln \frac{1}{\theta} + E_c \right) = \theta(A - B \ln \theta) \qquad (2.5)$$

where $A = E_c / b$ and $B = \mu b / 4\pi(1-\nu)$. Comparing the energies obtained by calculation with equation 2.4 to experimental data [7] proves the validity of this dislocation model, as the energy increase with increasing angle of rotation θ is predicted, accordingly, for angles $\theta < 15°$ [1].

1.4.2. High angle grain boundaries

For rotation angles larger than 15°, the lattice dislocation model no longer applies, as the dislocation cores are brought to an overlapping [8], causing the loss of their identity as individual lattice defects. Therefore, grain boundaries with rotation angles larger than 15° are distinguished from LAGBs and are

termed high angle grain boundaries (HAGB). The current concept of the structure of HAGBs was deduced from geometrical considerations, based on dislocation models for LAGBs and atomistic simulations [5, 7, 9, 1].

Most commonly, the structure of interfaces is described by the coincidence site lattice (CSL)- displacement shift complete (DSC) lattice construction. The atomic arrangement in a perfect crystal is determined by the minimum of free energy and any deviation of the former from ideal positions inevitably causes an increase of the latter [2]. Consequently, it is safe to assume that the atoms will remain close to their ideal position. At certain misorientations between two crystallites, crystallographic planes exist that transcend the grain boundary from one crystallite to the other, i. e. certain atomic positions in the grain boundary coincide with ideal positions in both neighboring crystallites. These atomic positions are termed coincidence sites and the super lattice containing these sites on the other hand is the aforementioned coincidence site lattice (CSL). The elementary cell of the CSL is self-evidently larger than the elementary cell of the crystal lattice and its volume may be calculated in terms of the lattice parameters of the crystal lattice. The CSL is characterized by the density of its coincidence sites, which in turn are defined by the quantity Σ [2]:

$$\Sigma = \frac{\text{volume of elementary cell CSL}}{\text{volume of elementary cell of crystal lattice}} \qquad (2.6)$$

Since coincidence sites are representations of atoms located at ideal fit positions, it is safe to assume that grain boundaries preferably stretch along coincidence sites [2].

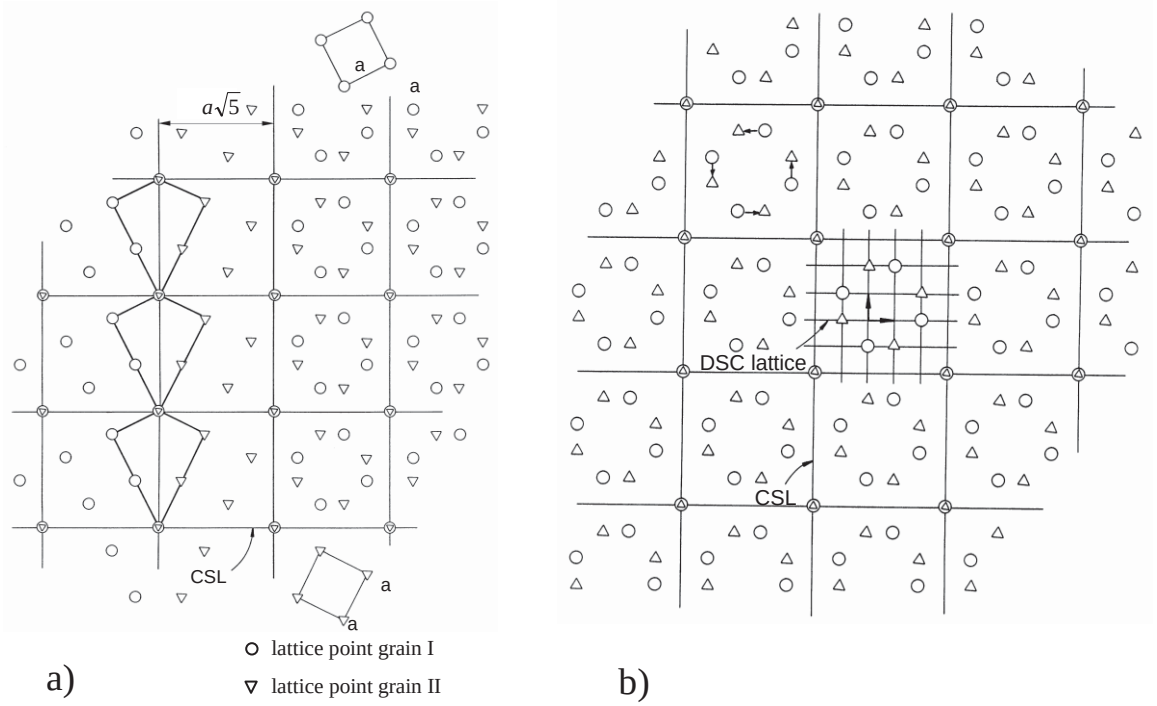

Fig. 1-5: **a) Coincidence site lattice (CSL) of a 36.87° <100> grain boundary (∑=5). Left: grain boundary plane is perpendicular to paper plane (tilt boundary). Right: grain boundary plane is parallel to paper plane (twist boundary). b) CSL and displacement shift complete lattice (DSC) at 36.87° <100> rotation in a cubic lattice. [1]**

Grain boundaries containing a high density of coincidence sites are called CSL boundaries or special boundaries. The order of the boundary increases with the decrease of the Σ–value, which is always an odd integer. Experimental data show that CSL grain boundaries of low Σ indeed consist of a low energy configuration, which is reflected by a low free surface energy [10, 11] and low grain boundary migration activation enthalpy [12]. However, there is a fundamental problem in applying this concept to real, arbitrary grain boundaries: since the CSL only exists at very special, defined angles and does not continually change with misorientation angle θ, the long range coincidence is lost even for small deviations [2]. This may be compensated by the introduction of dislocations with DSC Burgers vectors which are also referred to as

secondary grain boundary dislocations (SGBDs), as they are confined to the grain boundary [1].

Detailed analysis revealed that 7 different polyhedra (see. Fig. 1-6) are necessary to account for all possible arrangements of atoms in a grain boundary [13].

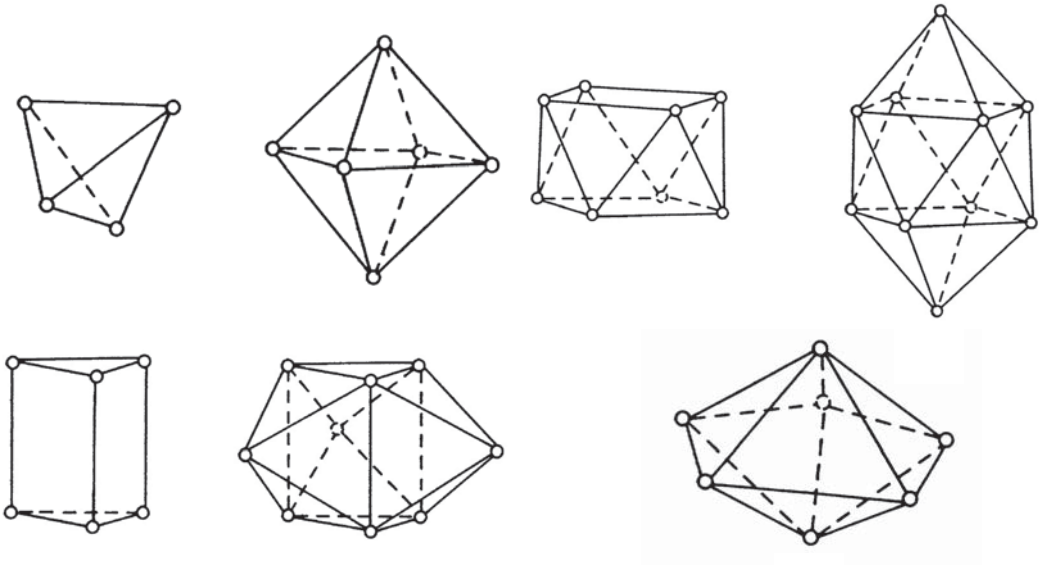

Fig. 1-6: The seven Bernal structures, of which the structural units of GBs are composed [13, 38].

These polyhedra represent characteristic structures of the grain boundary and are thus termed structural units. It has been shown by computer simulations, that low energy boundaries consist of only one type of structural unit [2]. Upon changing the orientation relationship, other structural units are introduced into the boundary plane, which are identical to the cores of SGBDs. The density of the newly introduced structural units increases with the grain boundaries misorientation angle, until eventually the grain boundary structure solely

consists of these new structural units. This concept of structural units constitutes our current understanding of grain boundary structures [1].

Analogously to the dislocation model of LAGBs, where the model by Read and Shockley [6] applies, the CSL-DSC model is no longer valid above a maximum deviation $\Delta\omega$ from exact CSL-misorientations, because the spacing of the SGBDs decreases with increasing deviation. As such, the SGBDs above a certain deviation of the misorientation angle tend to overlap and therefore lose their individuality. The most common criterion for the maximum deviation proposed by Brandon [15] reads:

$$\Delta\omega = \frac{15°}{\sqrt{\Sigma}} \tag{2-7}$$

Grain boundaries satisfying this criterion are referred to as special grain boundaries as opposed to random grain boundaries.

1.5. Classical model of grain boundary motion

Over the past 60 years, grain boundary motion has been subjected to extensive experimental and theoretical investigations. However, to this day no unified theory about grain boundary migration has been published, which were able to account for phenomena such as the misorientation dependence of grain boundary mobility as observed for instance by Aust and Rutter [16]. Basically, all theoretical attempts to describe grain boundary motion are based on the reaction rate theory by Smoluchoski [17] and Turnbull et al. [18], in which individual atoms cross the grain boundary accompanied by a net energy gain. It

is assumed that the detachment of one atom from a crystal to join the crystal across the boundary destroys a lattice site rather than creating a vacancy and that its attachment to the adjacent crystal surface generates a new lattice site as opposed to eliminating a vacancy [1].

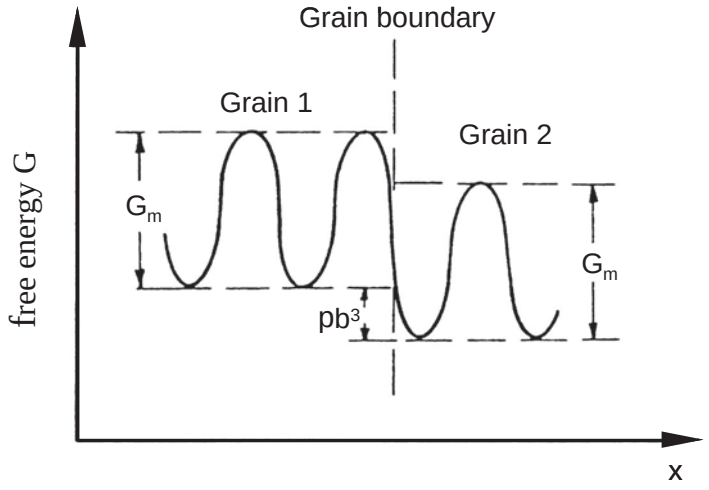

Fig. 1-7: The free energy G of a moving atom changes by the driving force pb^3 when it crosses the grain boundary. G_m is the free energy barrier for bulk diffusion [1].

Following these assumptions, grain boundary motion is conveniently simplified to diffusive motion of single atoms across the boundary rather than the uniform motion of atom groups.

We shall now derive the rate equation for grain boundary velocity, as seen in Ref. [1]: for the simplest case, the grain boundary is assumed to have a thickness of a monatomic layer, hence the boundary may be crossed by a single atomic jump and each transferred atom displaces the boundary by the diameter of an atom. Grain boundary velocity v is then expressed by [19]

$$\mathrm{v} = b\left(\Gamma_+ - \Gamma_-\right) \tag{2.8}$$

where Γ_+ and Γ_- are the jump frequencies in opposite directions, respectively. In case of zero difference in Gibbs free energy between the two grains, the net flux will also equal zero. However, any difference in Gibbs free energy per unit volume gives rise to a driving force *p*:

$$p = -\frac{dG}{dV} \tag{2.9}$$

In that case, each atom attaching to the growing grain of volume $\Omega^3 \approx b^3$ will gain the energy pb^3. The change in Gibbs free energy associated with this process is schematically shown in Fig. 1-7. The grain boundary velocity then reads:

$$\mathrm{v} = b\left(\nu_+ \exp\left(-\frac{G_m^+}{kT} \right) - \nu_- \exp\left(-\frac{G_m^- + pb^3}{kT} \right) \right) \tag{2.10}$$

The assumption of equal jump frequencies $\nu_+ = \nu_- = \nu_D$ (ν_D – Debye-frequency) and equal migration free energy G_m for both jump directions simplifies the equation to

$$\mathrm{v} = b\,\nu_D \exp\left(-\frac{G_m}{kT} \right)\left(1 - \exp\left(-\frac{pb^3}{kT} \right) \right) \tag{2.11}$$

Further assuming that $pb^3 << kT$ for $T \geq 0.3T_m$, a series expansion of the second exponential term

$$\exp\left(-\frac{pb^3}{kT}\right) \cong 1 - \frac{pb^3}{kT} \tag{2.12}$$

finally yields for velocity v

$$\mathrm{v} = \frac{b^4 \nu_D}{kT} \exp\left(-\frac{G_m}{kT}\right) \cdot p \equiv m \cdot p \tag{2.13}$$

where m is referred to as grain boundary mobility, the proportionality factor of the fundamental linear relationship between grain boundary velocity and driving force. Variable m basically contains all the kinetic characteristics of the grain boundary. Furthermore, it is also distinguished between the intrinsic mobility determined by grain boundary misorientation and inclination and the extrinsic mobility primarily governed by impurity content and dislocation densities.

By introducing the Nernst-Einstein relation for general diffusive processes (volume diffusion, grain boundary diffusion, etc.) without specification into the equation, the relation between grain boundary mobility and diffusion of atoms across the boundary reads:

$$m = \frac{b^2 D_m}{kT} = m_0 \cdot \exp\left(-\frac{H}{kT}\right) \tag{2.14}$$

D_m is the diffusion coefficient for diffusion jumps through the boundary, m_0 and H are the pre-exponential factor and activation enthalpy of the grain boundary mobility. This simple model may be modified by assuming the detachments to occur in a sequence of steps or thermal grain boundary vacancies to assist diffusion [20]. However, these modifications will only affect the pre-exponential factor m_0 and the activation enthalpy H of mobility m leaving the migration rate v and the driving force p unaffected [1].

1.6. Driving forces of grain boundary migration

The driving force p is a force acting per unit area on a grain boundary and its source may be of various origins. Generally, a driving force emerges when the motion of a grain boundary results in reducing the system's overall free energy. A gradient of any intensive thermodynamic variable offers a source of such driving forces: temperature gradients, pressure, density of defects, energy density (elastic, magnetic, electrical), etc. A more detailed treatise on the various driving forces utilized in grain boundary migration experiments was written by Gottstein and Shvindlerman [1].

1.6.1. Magnetic driving force

We shall now take a detailed look at the magnetic driving force, which was predominantly applied to induce grain boundary migration in the experiments featured in this work. Mullins was the first to use the driving force induced by a

high magnetic field to induce grain boundary migration in bismuth polycrystals [21].

Due to its anisotropic properties, zinc possesses a different magnetic susceptibility parallel ($\chi_{||}$) and perpendicular ($\chi_{\perp}$) to its hexagonal or *c*-axis such that $|\chi_{||}|>|\chi_{\perp}|$. The susceptibility tensor is represented by:

$$\underline{\underline{\chi}} = \begin{pmatrix} \chi_{\perp} & 0 & 0 \\ 0 & \chi_{\perp} & 0 \\ 0 & 0 & \chi_{||} \end{pmatrix} \tag{2.15}$$

As shown schematically in Fig. 1-8 below, the susceptibility tensor surface for zinc has an ellipsoidal shape.

Therefore, inside a magnetic field a driving force for grain boundary motion is induced between two crystallites due to a difference of magnetic free energy density ω, which is given by

$$\omega = \int_0^H \mu_0 \left(\vec{H} + \vec{M}\right) d\vec{H} = \mu_0 \frac{H^2}{2} \left(1 + \sum \chi_{ij} l_i l_j\right) \tag{2.16}$$

where μ_0 is the vacuum permeability and $\vec{H}$ is the magnetic field strength. The magnetic polarization specific to the material is given by $\vec{M} = \underline{\underline{\chi}} \cdot \vec{H}$ (see eq. 2.15) and $l_s = cos\Theta_s$ are the cosines between the principal crystal axes and the magnetic field $\vec{H}$.

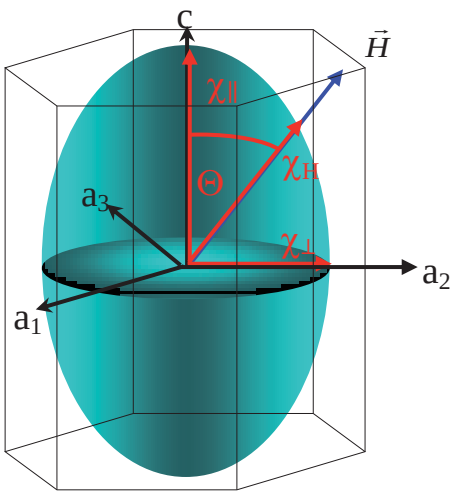

Fig. 1-8: Schematic depiction of the anisotropy of magnetic susceptibility in zinc, with respect to the unit cell. The spatial dependence of the magnetic susceptibility may be described by a second rank tensor and is represented by an ellipsoidal surface [22].

As shown analogously in Ref. [22] for other anisotropic crystal properties, we shall in the following develop a general expression for the magnetic driving force. Taking into account, that there are only two independent susceptibility components in zinc, equation 2.16 reduces to:

$$\omega = \mu_0 \frac{H^2}{2}\left(1+\chi_{\perp}\left(l_1^2+l_2^2\right)+\chi_{\parallel}l_3^2\right) \tag{2.17}$$

which since

$$l_1^2+l_2^2+l_3^2=1 \Rightarrow l_1^2+l_2^2=1-l_3^2 \tag{2.18}$$

may be further simplified to:

$$\omega = \mu_0 \frac{H^2}{2}\left(1+\chi_\perp+\left(\underbrace{\chi_{||}-\chi_\perp}_{\Delta\chi}\right)\cos^2\Theta_3\right) \qquad (2.19)$$

Thus, a general expression is obtained for the magnetic free energy density ω associated with a given orientation of a zinc crystal in an external magnetic field, dependent on only one spatial variable, Θ_3, the angle between the crystallographic c-axis and magnetic field vector $\vec{H}$. To calculate the driving force for magnetically induced grain boundary motion *p*, the magnetic free energy density associated with the two orientations of the crystallites in the magnetic field separated by the grain boundary have to be subtracted from one another, which finally results in:

$$p = \omega_1 - \omega_2 = \mu_0 \frac{H^2}{2}\Delta\chi\left(\cos^2\Theta_1 - \cos^2\Theta_2\right) \qquad (2.20)$$

where Θ_1 and Θ_2 are the angles between the *c*-axes in both neighboring crystallites and the magnetic field $\vec{H}$. The susceptibility difference in Zn was measured to be $\Delta\chi = 0.5\cdot10^{-5}$ and found not to depend on the temperature [23]. Now that the driving force for bicrystalline samples was deduced, we will proceed to magnetic driving forces in polycrystals: as applied in [24, 25], the magnetic driving force for the growth of each grain in a polycrystal is given by equation 2.21 below. Like discussed above for the case of bicrystalline samples, the crystallites with energetically favorable c-axis orientation with respect to the field are bound to grow while the crystallite with a less favorable orientation

will shrink. This is caused by the differing magnetic susceptibility in zinc parallel and perpendicular to its crystallographic c-axis. Equation 2.21, as introduced in Ref. [24], describes the magnetic driving force acting on one grain in a polycrystal,

$$p_m = \omega - \overline{\omega} = \frac{\mu_0 H^2}{2}\left(\chi - \frac{1}{n}\sum_j^n \chi_j\right) = \frac{1}{2}\mu_0 \Delta\chi H^2 \left(\cos^2\Theta - \frac{\sum_j^n \cos^2\Theta_j}{n}\right) \quad (2.21)$$

where Θ and Θ_j are the angles between field direction and the principal axes of the grain considered and its n neighboring grains. If $\Delta\chi > 0$ (which is true for Zn) and the condition $\cos^2\Theta - 1/n \cdot \sum_n \cos^2\Theta_n < 0$ is met by the one grain and its adjacent grains, the magnetic energy density ω in the one grain is lower than the average energy density of its neighboring grains ($\omega < \overline{\omega}$). Thus, the magnetic driving force promotes growth of the former grain, as then $p_m < 0$ [24].

The largest obtainable driving force is governed by the magnetic field strength at disposal and the magnetic susceptibility difference $\Delta\chi$ of the material under investigation. In the case of zinc, the maximum driving force p_m is calculated to 1.2 kJ/m^3 in high field magnets with a maximum field strength of 25 Tesla. Considering the applicability for grain boundary migration experiments, two major advantages over the capillary driving force (see section 1.6.2 below) are:

1.) The magnetic driving force facilitates the addressing of absolute grain boundary mobility as opposed to reduced mobility, thus enabling the migration measurements of crystallographically defined grain boundaries and studying the inclination dependence of activation parameters.
2.) The possibility to adjust the magnitude of the driving force during the experiment.

Curvature driven migration experiments do not yield the absolute mobility as a result, as the grain boundary inclination changes along the curvature and with it, consequently, its structure.

Therefore, in curvature driven migration experiments one basically obtains the averaged mobility of a large set of differently inclined grain boundaries, rather than the absolute mobility of one spatially defined, planar boundary.

1.6.2. Capillary driving force

Unlike with grain growth induced by a magnetic driving force, where the free energy gain during grain boundary motion originates from the alignment of crystal volume swept by the boundary to an orientation associated with lower magnetic susceptibility, the capillary driving force is provided by the free energy of the grain boundary and stems from the pressure difference Δp, caused by the difference of capillary forces on both sides of a curved grain boundary [1]. The capillary pressure is expressed by:

$$\Delta p = \gamma \left(\frac{1}{R_1} + \frac{1}{R_2} \right) \tag{2.22}$$

where γ is the grain boundary free energy and R_1, R_2 are the main radii of curvature under the assumption of boundary isotropy. Upon thermal activation this driving force induces boundary motion in the direction towards the center of curvature, causing a reduction of grain boundary area and, consequently, energy. However, the use of the capillary driving force only permits to evaluate a reduced boundary mobility, $A = \gamma m$, where the grain boundary free energy is still part of the equation and thus factors into the obtained mobility values.